Available online at www.sciencedirect.com
ScienceDirect
Journal of Luminescence 127 (2007) 181–185
JOURNAL OF LUMINESCENCE
www.elsevier.com/locate/jlumin

Third-order nonlinear-optical parameters of gold nanoparticles in different matrices

A.I. Ryasnyanskiy[a,b,*], B. Palpant[a], S. Debrus[a], U. Pal[c], A. Stepanov[d]

[a]*Institut des Nano-Sciences de Paris, CNRS–Université Pierre et Marie Curie, Case 80, 140 rue de Lourmel, F75015 Paris, France*
[b]*Samarkand State University, 703004 Samarkand, Uzbekistan*
[c]*Instituto de Física, Universidad Autónoma de Puebla, Apdo. Postal J-48, Puebla, Pue. 72570, Mexico*
[d]*Kazan Physics-Technical Institute, Russian Academy of Sciences, 420029 Kazan, Russian Federation*

Available online 25 February 2007

Abstract

Third-order nonlinear-optical properties of gold nanoparticles embedded in Al_2O_3, ZnO and SiO_2 have been investigated by the *Z*-scan method at the wavelength of 532 nm using nanosecond Nd^{3+}:YAG laser radiation. The nonlinear refractive index, nonlinear absorption coefficient, and the real and imaginary parts of the third-order nonlinear susceptibility are deduced. The results of the investigation of nonlinear refraction using the off-axis *Z*-scan configuration are presented and the mechanisms responsible for the nonlinear response are discussed. The prevailing influence of the electronic Kerr effect over the possible thermo-optical contribution is demonstrated.

1. Introduction

Metal nanoparticle systems like metal-doped glasses or colloidal solutions are of considerable interest due to fast response time on laser excitation [1,2] and large value of the third-order nonlinear susceptibility, $\chi^{(3)}$, responsible for Kerr effect [3–6]. Optical nonlinearities of gold nanoparticles were the subject of numbers of investigations during the past decade. The different influence of nanoparticle morphology (size and shape), preparation method (ion implantation, RF-sputtering, chemical, sol–gel, etc.) together with laser radiation parameters (pulse duration, repetition rate, wavelength, etc.) on the nonlinear optical properties of materials were considered. The role of surrounding matrix characteristics was also the subject of numerous studies. Thus, for example, water [7–10], silicate glass [3–5], $BaTiO_3$ [11], Al_2O_3 [12,13], $LiNbO_3$ [14], TiO_2 [15] were applied for composite material optimization to obtain appropriate values of the nonlinear optical coefficients.

An important characteristic for practical material application is the sign of the nonlinear refractive coefficient, γ. It can be positive, when material behaves like a focusing lens, and negative in the case where material diverges laser radiation. The sign of the nonlinear refractive index depends on both laser characteristics and material ones.

Among the methods used for the investigation of nonlinear optical parameters of materials are the optical phase conjugation [1], degenerate four-wave mixing (DFWM) [15], nonlinear interferometry [17], and also one of the most comfortable and informative technique—the *Z*-scan technique [18]. The latter allows determination of both the value and the sign of nonlinear optical parameters (nonlinear refraction and absorption coefficients), and that is an advantage over other methods such as DFWM, that allows the measurement of the modulus of $\chi^{(3)}$ only. Note that the DFWM technique was previously applied for the determination of $|\chi^{(3)}|$ of $Au:Al_2O_3$ materials in the vicinity of the SPR of gold nanoparticles, but neither the imaginary and real parts of $\chi^{(3)}$ nor their sign could be measured [15].

In this paper the *Z*-scan technique was used for the determination of the value and the sign of the imaginary

*Corresponding author. Samarkand State University, 703004 Samarkand, Uzbekistan. Tel.: +998662295382; fax: +998662333441.
E-mail address: ryasn2000@yahoo.com (A.I. Ryasnyanskiy).

0022-2313/$ - see front matter © 2007 Elsevier B.V. All rights reserved.
doi:10.1016/j.jlumin.2007.02.021

and real parts of the third-order nonlinear susceptibility of gold nanoparticles in Al_2O_3, ZnO and SiO_2.

2. Structural and optical characteristics of the samples

The samples with gold nanoparticles have been synthesized by radiofrequency (RF) magnetron sputtering technique. The detailed descriptions of preparation procedures are given in Ref. [19] for Al_2O_3, in Ref. [20] for ZnO and in Ref. [6] for SiO_2. In Table 1, the structural characteristics of the investigated samples are collected. Analysis of the absorption spectra of gold nanoparticles in three matrices showed that SPR of gold nanoparticles are located in the region of 525 nm for Al_2O_3 [19], 540 nm for ZnO [20] and 500 nm for SiO_2 [6].

3. Nonlinear optical measurements

A frequency-doubled Q-switched Nd^{3+}:YAG laser (pulse duration: 7 ns, wavelength: 532 nm, repetition rate: 10 Hz) was used for the *Z*-scan experiments. The detailed description of the experimental set-up is given in Ref. [21], with an additional improvement consisting of adding a second reference arm having exactly the same optical path as the closed-aperture detection arm, except from the sample, in order to reduce the detection noise stemming from pulse-to-pulse beam pointing fluctuations, as proposed in Ref. [22]. The peak intensity (I_{00}) range was 1×10^6–2×10^6 W/cm^2 that was below the optical breakdown threshold for the samples investigated. As the linear absorption of the samples studied was quite high, much attention was given during the experiments to prevent material optical breakdown and irreversible changes produced by laser radiation [23,24]. The present experiments were carried out at different radiation intensities for several times at the same point on the sample surface to ensure that there were no structural changes in materials, what was confirmed by a good reproducibility of the results obtained.

The closed-aperture *Z*-scan scheme [18] allows determination of the sign and the magnitude of the sample nonlinear refractive index. The results of the measurements of three samples are presented in Fig. 1. It is seen that the sign of γ is positive (valley-peak profile [18]) for gold nanoparticles in Al_2O_3 (Fig. 1a) and SiO_2 (Fig. 1b) and negative for gold in ZnO (Fig. 1c). The results regarding the nonlinear refraction coefficient γ and $\mathrm{Re}\chi^{(3)}$ are collected in the Table 2.

Table 1
Morphological and optical characteristics of the Au:Al_2O_3 samples

Matrix	Metal concentration (%)	Film thickness (nm)	Mean nanoparticles size (nm)
Alumina	8	117	3.1
SiO_2	8	141	2.6
ZnO	8.68	930	

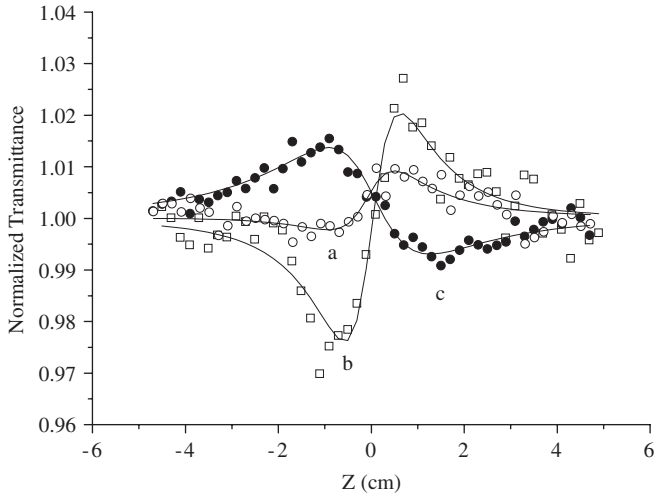

Fig. 1. *Z*-scan profiles of the normalized transmittance measured for Au:Al_2O_3 (a), Au:SiO_2 (b) and Au:ZnO (c) in the closed-aperture scheme. Solid lines are theoretical fits to the experimental data. Note that the peak intensity is different from one curve to the other: $I_{00}=5.7$ MW cm^{-2} (a), 28 MW cm^{-2} (b) and 8 MW cm^{-2} (c).

The *Z*-scan scheme with an open aperture [18] was used for the investigation of the nonlinear absorption process in the samples. The results of the measurements are presented in Fig. 2. One can see that the nonlinear absorption coefficient β is negative, signing an absorption saturation process in Au:Al_2O_3 and Au:SiO_2. For the sample Au:ZnO nonlinear absorption signal was not observed. The calculated values of β and the imaginary parts of $\chi^{(3)}$ are also presented in Table 2.

4. Discussion

Let us first consider the influence of nonlinearities of pure matrices on the nonlinearity of the investigated composite materials. Note, that experiments with pure matrices did not show any signal demonstrating refraction or absorption nonlinearities at the intensities used. The values of γ reported for matrices under consideration are 3.3×10^{-16} cm^2 W^{-1} for Al_2O_3 [25], -9×10^{-15} cm^2 W^{-1} for ZnO [26] and 2.24×10^{-16} cm^2 W^{-1} for SiO_2 [27] at the wavelength of 532 nm. These data are much smaller than that of the composite materials and therefore one can conclude that the nonlinear optical response of the investigated composite materials originates from gold nanoparticles. We will now consider the possible mechanisms of nonlinear refraction in our samples.

A considerable contribution to the nonlinear refractive index can stem from a thermal lensing effect, which can be considered as a result of energy transfer from heated metal nanoparticles to the whole medium [28]. Time which is necessary for this process to be settled (t_{tl}) is determined by the ratio of the focused laser beam radius (w_0) to the value of the sound velocity in the dielectric matrix (v). Taking into account our experimental conditions ($w_0=35$ μm for Au in Al_2O_3 and SiO_2 and $w_0=45$ μm for Au:ZnO) both

Table 2
Nonlinear optical characteristics of gold nanoparticles

Matrix	β (10^{-3} cm W^{-1})	Im$\chi^{(3)}$ (10^{-7} esu)	γ (10^{-9} cm^2 W^{-1})	Re$\chi^{(3)}$ (10^{-7} esu)	$\lvert\chi^{(3)}\rvert$ (10^{-7} esu)	$\lvert\chi^{(3)}_m\rvert$ (10^{-8} esu)
Alumina	−1.31	−5.33	7.62	5.03	7.33	6.25
SiO_2	−0.12	−0.067	2.97	1.38	1.38	2.7
ZnO	<0.08	<0.044	−1.31	−1.47	1.47	2.46

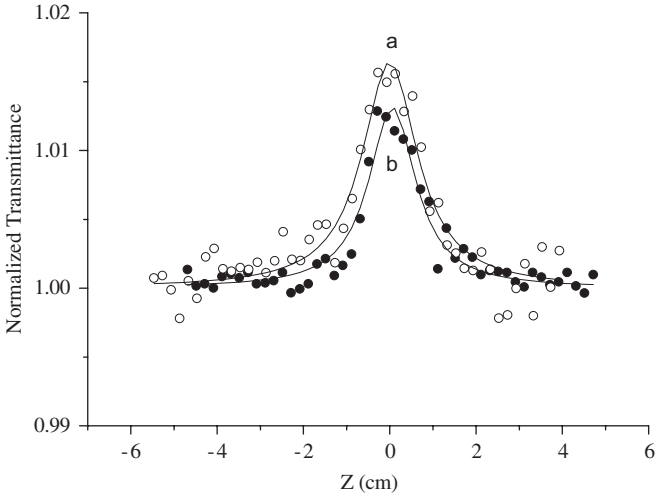

Fig. 2. *Z*-scan profiles of the normalized transmittance measured for Au:Al_2O_3 (a) and Au:SiO_2 (b) in an open-aperture scheme. Solid lines are theoretical fits to the experimental data. Note that the peak intensity is different from one curve to the other: $I_{00} = 5.7\,\mathrm{MW\,cm^{-2}}$ (a) and $28\,\mathrm{MW\,cm^{-2}}$ (b).

with the values of sound velocity in the matrices used ($v = 6700\,\mathrm{m\,s^{-1}}$ for Al_2O_3 [29], $6590\,\mathrm{m\,s^{-1}}$ for ZnO [30] and $5939\,\mathrm{m\,s^{-1}}$ for SiO_2) the value of t_{tl} were calculated to be 5.2, 5.8 and 5.9 ns, respectively. These times are very close to the value of pulse duration used in the experiment ($\tau = 7$ ns). This shows the importance of thermal effect to be taken into account when considering the origin of the nonlinearities observed. It should be also noted that it is possible to generate a cumulative thermal effect if high repetition rate lasers are used (kHz or MHz [31]). However, in our experiments laser radiation with a low repetition rate (10 Hz) was used, thus preventing the appearance of such a cumulative effect.

To analyze the mechanisms responsible for nonlinear refraction in investigated samples the measurement of the time-dependence of the signal transmitted through the sample and the aperture in the off-axis scheme, by using fast photodiode detectors (response time: ~500 ps). This method was applied earlier in experiments with colloidal gold [28], where the temporal and amplitude shift of the transmitted pulse maximum was observed. The experimental conditions were the same as those used for the results of Fig. 1 except the aperture position with respect to the optical beam axis. The aperture was shifted to the radial distance of 4–5 mm. The sample was kept at the position z of maximum transmission (Fig. 1). The signal and reference (proportional to the incident pulse) oscilloscope traces are presented in Fig. 3. One can see that the only change concerns the amplitude of the transmitted pulse, without any temporal shift of the maximum. This allows us to conclude that the third-order nonlinear response of investigated materials was due to prevailing influence of pure electronic effect. As a pure electronic Re$\chi^{(3)}$ is frequency dependent and its sign depends on the correspondence between SPR maximum and the wavelength of radiation used, SPR location for three matrices is different and for alumina and SiO_2 it is above the wavelength of laser radiation and for ZnO it is below. We think it is the reason why the sign of Re$\chi^{(3)}$ is positive for alumina and SiO_2, and negative for ZnO.

Let us now examine the intrinsic nonlinear susceptibility of the gold nanoparticles $\chi^{(3)}_m$ [16]:

$$\chi^{(3)} = p|f^2|f^2\chi^{(3)}_m, \tag{1}$$

where f is the local field factor, which can be expressed for an isolated metal particle surrounded by a dielectric matrix, as

$$f = \frac{3\varepsilon_d}{\varepsilon_m + 2\varepsilon_d}, \tag{2}$$

where ε_d and ε_m are the dielectric functions of the matrix and the metal, respectively. Eq. (2) can be applied for materials having a low metal concentration, like our present samples ($p \cong 8\%$). Indeed, while it has already been shown that with increasing metal amount the local field factor diverges from the value given by Eq. (2), the discrepancy remains weak in the case of a Au:SiO_2 medium with $p = 8\%$ [32–34]. We suppose that this is also the case for Au:Al_2O_3 and Au:ZnO. Note that the possible influence of quantum size effects on the value of ε_m will be disregarded here, as we just aim at extracting the order of magnitude of the complex value of $\chi^{(3)}_m$ from our experiments. From the values of Im$\chi^{(3)}$ and Re$\chi^{(3)}$, the value of $|\chi^{(3)}|$ was calculated (see table 2). Using Eqs. (1) and (2) at $\lambda = 532$ nm, we calculated also the modulus of the intrinsic nonlinear susceptibility of metal nanoparticles. These results are also included in Table 2. It should be noted that obtained results are in good agreement with other values found in the literature (5×10^{-8} esu for Au:SiO_2 [16], $2–4 \times 10^{-8}$ esu for Au:H_2O [35]).

As one can see from Table 2, for Au nanoparticles in alumina, both imaginary and real parts of $\chi^{(3)}$ have approximately the same contributions to $\chi^{(3)}$, but for other samples the value of $\chi^{(3)}$ is mostly real. The possible reason for this is that the wavelength used is closer to SPR of Au nanoparticles in alumina than SPR of Au nanoparticles in

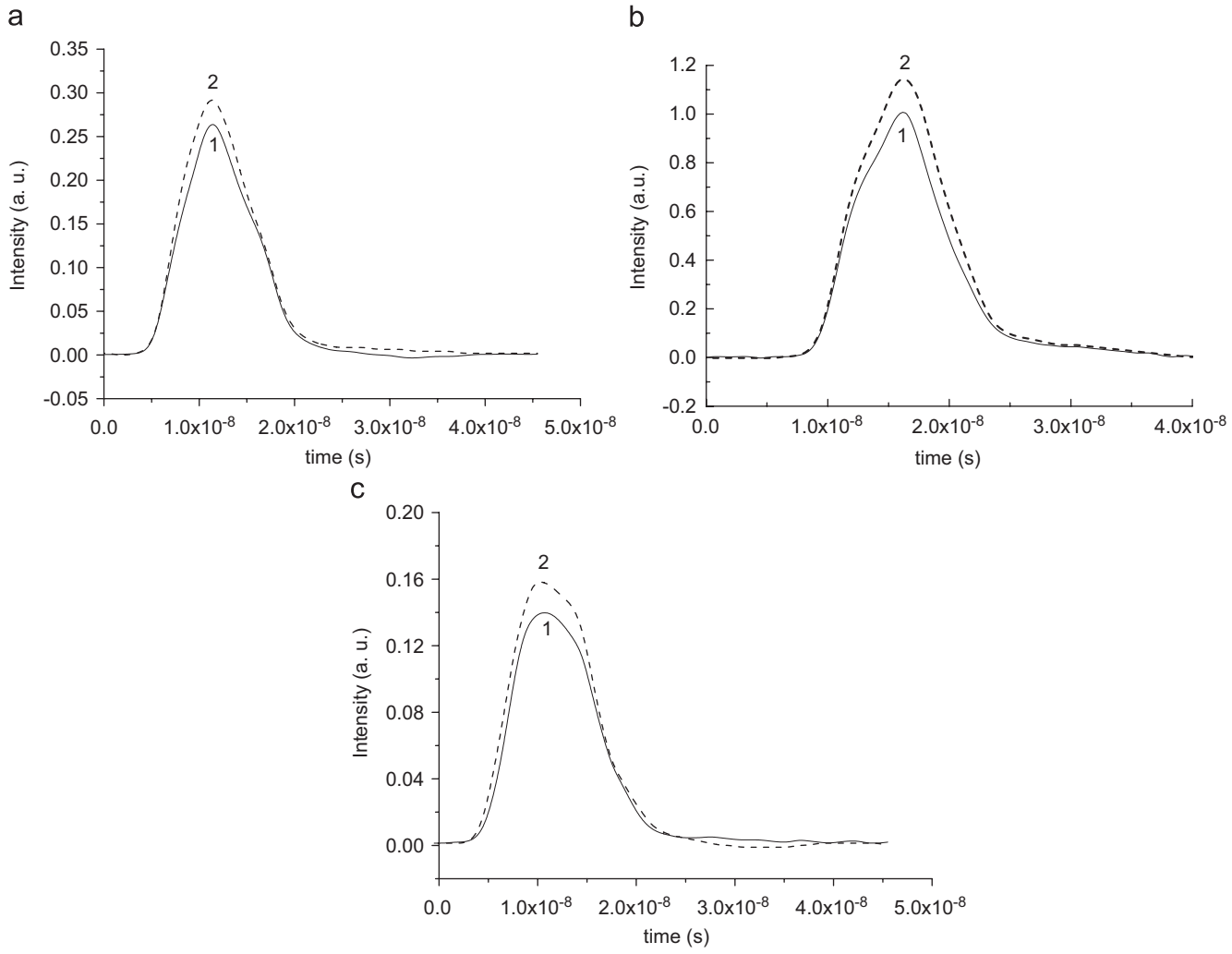

Fig. 3. Temporal profiles of the pulses transmitted through the sample (2) and off-axis aperture with respect to the temporal profiles of the reference pulses (1) for Au:Al_2O_3 (a), Au:SiO_2 (b) and Au:ZnO (c).

other two matrices. It leads to the higher linear absorption in Au:alumina sample and, respectively, higher absorption saturation process. Additional investigation will be done to clarify the question of absence of absorption saturation in Au:ZnO.

5. Conclusion

The optical nonlinearities of composite materials with gold nanoparticles have been measured by the *Z*-scan technique using nanosecond radiation of a pulsed Nd^{3+}:YAG laser at $\lambda = 532$ nm. The real and imaginary parts of the material third-order nonlinear susceptibilities and the modulus of the third-order nonlinear susceptibility of particles themselves have been deduced. The temporal analysis of the radiation transmitted through the samples showed the prevailing influence of pure electronic origin of the third-order nonlinearities measured in this paper. The values of $|\chi_m^{(3)}|$ measured in this paper are in a good agreement with those measured by other authors.

Acknowledgements

A.I.R. acknowledges the financial support of the NATO foundation (Grant N 981559). A.L.S. is grateful to the Alexander Humboldt Foundation (Germany) and the Austrian Scientific Foundation in the frame of Lise Meitner program for the financial support. This study was sponsored partly by the Federal Program for Support of the Leading Scientific Schools of Russian Federation (Grant no. NSh 1904.2003.2), the Russian Foundation for basic Research (Grant no. 04-02-97505 and Grant no. 06-02-08147-ofi), the OFN of Russian Academy of Sciences ''Advanced Materials and Structures'' and also CONACyT (Grant no. 46269), Mexico.

References

[1] T. Tokizaki, A. Nakamura, S. Kaneko, K. Uchida, S. Omi, H. Tanji, Y. Asahara, Appl. Phys. Lett. 65 (1994) 941.
[2] H. Inouye, K. Tanaka, I. Tanahashi, Y. Kondo, K. Hirao, J. Phys. Soc. Jap. 68 (1999) 3810.

[3] R.A. Ganeev, A.I. Ryasnyansky, A.L. Stepanov, T. Usmanov, Phys. Stat. Sol. B. 241 (2004) R1.
[4] R.A. Ganeev, A.I. Ryasnyansky, A.L. Stepanov, T. Usmanov, Phys. Stat. Sol. B. 4 (2004) 935.
[5] R.A. Ganeev, A.I. Ryasnyanskiy, A.L. Stepanov, T. Usmanov, Opt. Quant. Electron. 36 (2004) 949.
[6] N. Pinçon, B. Palpant, D. Prot, E. Charron, S. Debrus, Eur. Phys. J. D 19 (2002) 395.
[7] R.A. Ganeev, M. Baba, A.I. Ryasnyasnky, M. Suzuki, H. Kuroda, Opt. Commun. 240 (2004) 437.
[8] L. Francois, M. Mostafavi, J. Belloni, J.F. Delouis, J. Delaire, P. Feneyrou, J. Phys. Chem. B. 104 (2000) 6133.
[9] R.A. Ganeev, A.I. Ryasnyansky, Sh.R. Kamalov, N.V. Kamanina, I.A. Kulagin, M.K. Kodirov, T. Usmanov, Nonlin. Opt. 28 (2002) 263.
[10] R.A. Ganeev, A.I. Ryasnyansky, S.R. Kamalov, M.K. Kodirov, T. Usmanov, J. Phys. D: Appl. Phys. 34 (2001) 1602.
[11] G. Yang, W.-T. Wang, G.-Z. Yang, Z.-H. Chen, Chin. Phys. Lett. 20 (2003) 924.
[12] J.M. Ballesteros, R. Serna, J. Solis, C.N. Afonso, A.K. Petford-Long, D.H. Osborne, R.F. Haglung Jr., Appl. Phys. Lett. 71 (1997) 2445.
[13] R.A. Ganeev, A.I. Ryasnyansky, A.L. Stepanov, C. Marques, R.C. da Silva, E. Alves, Opt. Commun. 253 (2005) 205.
[14] S.S. Sarkisov, E. Williams, M. Curley, D. Ila, P. Venkateswarlu, D.B. Poker, D.K. Hensley, Nucl. Instr. Meth. Phys. Res. 141 (1998) 294.
[15] H.B. Liao, R.F. Xiao, J.S. Fu, H. Wang, K.S. Wong, G.K.L. Wong, Opt. Lett. 23 (1998) 388.
[16] F. Hache, D. Ricard, C. Flytzanis, U. Kreibig, Appl. Phys. A 47 (1988) 347.
[17] M.J. Morgan, C.Y. She, R.L. Carman, IEEE J. Quant. Electron. 11 (1975) 259.
[18] M. Sheik-Bahae, A.A. Said, T.-H. Wei, D.J. Hagan, E.W. Van Stryland, IEEE J. Quant. Electron. 26 (1990) 760.
[19] A. Dakka, J. Lafait, C. Sella, S. Rerthier, M. Abd-Lefdil, J.-C. Martin, M. Maaza, Appl. Opt. 39 (2000) 2745.
[20] U. Pal, E. Aguila Almanza, O. Vázquez Cuchillo, N. Koshizaki, T. Sasaki, S. Terauchi, Sol. Energ. Mat. Sol. C. 70 (2001) 363.
[21] S. Debrus, J. Lafait, M. May, N. Pinçon, D. Prot, C. Sella, J. Venturini, J. Appl. Phys. 88 (2000) 4469.
[22] H. Ma, A.S.L. Gomes, C.B. de Araujo, Appl. Phys. Lett. 59 (1999) 2666.
[23] R. Serna, J.M. Ballesteros, J. Solis, C.N. Afonso, D.H. Osborne, R.F. Haglung Jr., A.K. Petford-Long, Thin Solid Films 318 (1998) 96.
[24] D.H. Osborne, R.F. Haglund, F. Gonella, F. Garrido, Appl. Phys. B. 66 (1998) 517.
[25] R. Adair, L.L. Chase, S.A. Payne, Phys. Rev. B. 39 (1989) 3337.
[26] R. De Salvo, A.A. Said, D.J. Hagan, E.W. Van Stryland, M. Sheik-Bahae, IEEE J. Quant. Electr. 32 (1996) 1324.
[27] X.J. Zhang, W. Ji, S.H. Tang, J. Opt. Soc. Am. B. 14 (1997) 1951.
[28] S. Mehendale, S.R. Mishra, K.S. Bindra, M. Laghate, T.S. Dhami, K.S. Rustagi, Opt. Comm. 133 (1997) 273.
[29] The value of the longitudinal sound velocity in amorphous Al_2O_3 synthesized by RF-sputtering was measured by B. Perrin and co-workers (private communication).
[30] D.C. Look, Sem. Sci. Tech. 20 (2005) 355.
[31] M. Falconieri, G. Salvetti, E. Cattaruza, F. Gonella, G. Mattei, P. Mazzoldi, M. Piovesan, G. Battaglin, R. Polloni, Appl. Phys. Lett. 73 (1998) 288.
[32] M. Rashidi-Huyeh, B. Palpant, J. Appl. Phys. 96 (2004) 4475.
[33] G.A. Swartzlander, B.L. Justus, A.L. Huston, A.J. Campillo, C.T. Law, Int. J. Nonlin. Opt. Phys. 2 (1993) 577.
[34] D. Prot, D.B. Stout, J. Lafait, N. Pinçon, B. Palpant, S. Debrus, J. Opt. A: Pure Appl. Opt. 4 (2002) S99.
[35] M.J. Bloemer, J.W. Haus, P.R. Ashley, J. Opt. Soc. Am. B 7 (1990) 790.